Structural and Molecular Orbital Study of the Furazan *N*-Oxide System. Structures of 3-Amino-4-methylfurazan *N*-Oxide and 4-Amino-3-methylfurazan *N*-Oxide, and Molecular Orbital Calculations

Piero Ugliengo and Davide Viterbo *
Istituto di Chimica Fisica dell' Università, Via P. Giuria 7, 10125 Torino, Italy
Mariano Calleri
Dipartimento di Scienze della Terra, Via San Massimo 24, 10123 Torino, Italy

The molecular structure of the two title furazan oxide isomers has been determined by three-dimensional *X*-ray analysis from diffractometer data. Molecular orbital calculations at *ab-initio* level, using minimal and split valence basis sets and at semiempirical level using the MINDO/3 approach, have been performed on 3-amino-4-methylfurazan *N*-oxide, 4-amino-3-methylfurazan *N*-oxide, 3-methyl-4-aminofurazan, 3,4-diaminofurazan, and unsubstituted furazan and furazan *N*-oxide. The influence of the amino substituent on the five-membered ring has been analysed; all results show that significant electronic effects are present.

As part of a systematic study on the structural and electronic properties of furazan *N*-oxide (furoxan) derivatives (*cf.* ref. 1), we have undertaken the *X*-ray analysis of the two amino-(methyl)furazan *N*-oxide isomers.

Recent interest in these compounds, and in related furazan derivatives, has arisen from their use as 'urea equivalent' groups within new histamine H_2-receptor antagonists of the ranitidine family.[2] In the present work, calculations have been carried out in order to gain a better understanding of the electronic interaction between the amino substituent and the furazan or furazan *N*-oxide ring.

The convention adopted previously [1] is adopted, in that the N atom of the *N*-oxide function is regarded as the 2-position; thus the isomers are indicated as 4-amino-3-methyl- (**1A**) and 3-amino-4-methyl-furazan *N*-oxide (**1B**), respectively.

X-Ray Study.—Final atomic parameters are listed in Tables 1 and 2 and bond distances and angles in Tables 3 and 4. Figures 1 and 2 show ORTEPII [3] views of the molecules together with the atom-labelling scheme.

The overall geometry of the five-membered ring in both isomers agrees with that found in other furazan *N*-oxide derivatives (*cf.* Table 9). The difference between the two C–N bonds is very small in both isomers, and that between the two nuclear N–O bonds is less pronounced than in other di-substituted furazan oxides and is smaller in (**1A**) (0.010 Å) than in (**1B**) (0.033 Å).

The exocyclic N ⟶ O bond is in both isomers longer [especially for (**1B**)] than in other derivatives. This lengthening can also be related to the formation of intermolecular hydrogen bonds involving O(2): in (**1A**) O(2)–N′(3) (at x, $1 + y$, z) is 3.026 Å [O(2)–H′(2) 2.14 Å], while in (**1B**), where the effect is more marked, O(2)–N′(3) (at $1 - x$, $-y$, $1 - z$) is 2.911 Å [O(2)–H′(1) 2.08 Å] and O(2)–N′(3) (at $x - \frac{1}{2}$, $\frac{1}{2} - y$, $z - \frac{1}{2}$) is 2.983 Å [O(2)–H′(2) 2.05 Å]. Furthermore an intramolecular interaction between O(2) and the amino group is present in (**1B**): O(2)–N(3) 2.921 Å, O(2)–H(1) 2.79 Å. On the other hand in (**1A**) a competing short contact is observed between N(3) and O(1): N(3)–O′(1) (at x, $1 + y$, z) is 3.041 Å [H(2)–O′(1) 2.56 Å].

In both isomers the five-membered ring is planar. In (**1A**) O(2), C(3) and N(3) do not deviate significantly from the ring plane. In (**1B**) only C(3) is on the ring plane while O(2) is 0.046 Å and N(3) is −0.022 Å out of the plane. In (**1A**) the amino group is rotated by 5.2° with respect to the ring plane; in (**1B**) this angle is 4.2°.

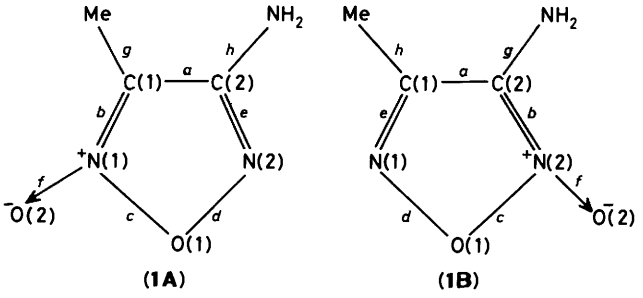

Table 1. Atomic co-ordinates ($\times 10^4$) and isotropic thermal parameters (Å^2 $\times 10^3$) for isomer (**1A**)

	x	y	z	U
O(1)	5 342(2)	9 542(1)	3 253(1)	57(1)[a]
O(2)	2 655(2)	8 353(2)	4 171(1)	64(1)[a]
N(1)	3 561(2)	9 907(2)	3 841(1)	46(1)[a]
N(2)	6 119(2)	11 474(2)	2 966(1)	54(1)[a]
N(3)	5 101(2)	14 874(2)	3 243(1)	63(1)[a]
C(1)	3 236(2)	11 891(2)	3 904(1)	42(1)[a]
C(2)	4 867(2)	12 832(2)	3 354(1)	43(1)[a]
C(3)	1 474(2)	12 781(2)	4 456(1)	55(1)[a]
H(1)	6 278(22)	15 314(27)	2 906(14)	69(4)
H(2)	4 218(25)	15 832(23)	3 551(14)	69(4)

Table 2. Atomic co-ordinates ($\times 10^4$) and isotropic thermal parameters (Å^2 $\times 10^3$) for isomer (**1B**)

	x	y	z	U
O(1)	5 004(1)	5 149(2)	2 163(2)	57(1)[a]
O(2)	4 182(1)	2 067(2)	3 213(1)	55(1)[a]
N(1)	6 143(2)	6 384(3)	2 586(2)	61(1)[a]
N(2)	5 140(1)	3 387(2)	3 334(1)	41(1)[a]
N(3)	6 732(1)	2 069(3)	5 594(2)	60(1)[a]
C(1)	6 904(1)	5 439(3)	3 872(2)	44(1)[a]
C(2)	6 297(1)	3 519(2)	4 361(2)	37(1)[a]
C(3)	8 221(2)	6 274(4)	4 661(3)	62(1)[a]
H(1)	6 312(18)	952(30)	5 827(21)	61(4)
H(2)	7 545(21)	2 492(31)	6 323(32)	61(4)

[a] Equivalent isotropic U defined as one third of the trace of the orthogonalized U_{ij} tensor.

Table 3. Bond lengths (Å) and angles (°) for isomer (**1A**)

O(1)–N(1)	1.416(2)	O(1)–N(2)	1.406(1)
O(2)–N(1)	1.248(2)	N(1)–C(1)	1.310(2)
N(2)–C(2)	1.307(2)	N(3)–C(2)	1.344(2)
C(1)–C(2)	1.425(2)	C(1)–C(3)	1.478(2)
N(1)–O(1)–N(2)	107.0(1)	O(1)–N(1)–O(2)	116.3(1)
O(1)–N(1)–C(1)	109.4(1)	O(2)–N(1)–C(1)	134.3(1)
O(1)–N(2)–C(2)	105.9(1)	N(1)–C(1)–C(2)	105.6(1)
N(1)–C(1)–C(3)	122.9(1)	C(2)–C(1)–C(3)	131.5(1)
N(2)–C(2)–N(3)	123.7(1)	N(2)–C(2)–C(1)	112.0(1)
N(3)–C(2)–C(1)	124.3(1)	C(2)–N(3)–H(1)	117.0(2)
C(2)–N(3)–H(2)	123.0(1)	H(2)–N(3)–H(1)	120.0(2)

Table 4. Bond lengths (Å) and angles (°) for isomer (**1B**)

O(1)–N(1)	1.384(2)	O(1)–N(2)	1.417(2)
O(2)–N(2)	1.272(2)	N(1)–C(1)	1.296(2)
N(2)–C(2)	1.309(2)	N(3)–C(2)	1.332(2)
C(1)–C(2)	1.425(2)	C(1)–C(3)	1.473(2)
N(1)–O(1)–N(2)	106.9(1)	O(1)–N(2)–O(2)	117.9(1)
O(1)–N(1)–C(1)	107.5(1)	O(2)–N(2)–C(2)	133.5(1)
O(1)–N(2)–C(2)	108.6(2)	N(1)–C(1)–C(2)	110.7(1)
N(1)–C(1)–C(3)	122.9(2)	C(2)–C(1)–C(3)	126.4(1)
N(2)–C(2)–N(3)	123.3(3)	N(2)–C(2)–C(1)	106.3(1)
N(3)–C(2)–C(1)	130.4(1)	C(1)–N(3)–H(1)	126.0(1)
C(1)–N(3)–H(2)	114.0(1)	H(2)–N(3)–H(1)	120.0(2)

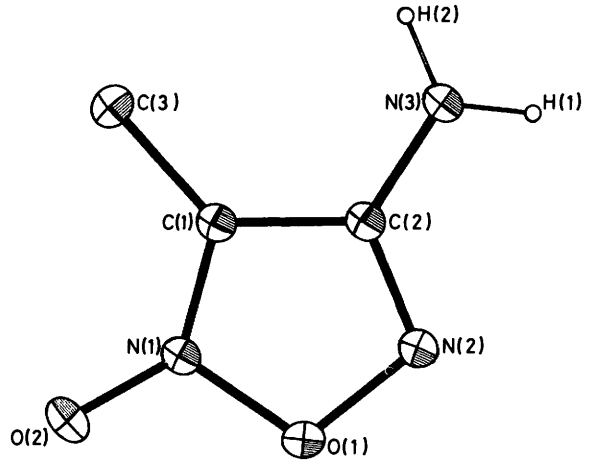

Figure 1. ORTEPII[3] projection of isomer (**1A**) on the plane through the five-membered ring; thermal ellipsoids are drawn at the 20% probability level

Theoretical Calculations.—Methods and aims. Theoretical semiempirical calculations using the MINDO/3 approach,[4] *ab initio* with minimal STO-3G,[5] and a split valence[6] 3-21G basis set have been performed on (**1A**), (**1B**), 3-amino-4-methylfurazan (**3**),[7] 3,4-diaminofurazan (**4**),[8] furazan (**5**),[9] and on furazan *N*-oxide itself (**6**) (see Figure 3). MINDO/3 calculations have been performed using the MOPAC package,[10] and *ab initio* calculations with GAUSSIAN80[11] and GAUSSIAN82.[12] The comparison of conformational studies on free molecules with *X*-ray data was aimed at obtaining a better insight into the balance between intramolecular and packing forces. A second aim was to compare the semiempirical results for (**1A**) and (**1B**) and related furazan derivatives with the *ab initio* results. The molecules of the pharmacologically important ranitidine analogues are too large for an *ab initio* approach.

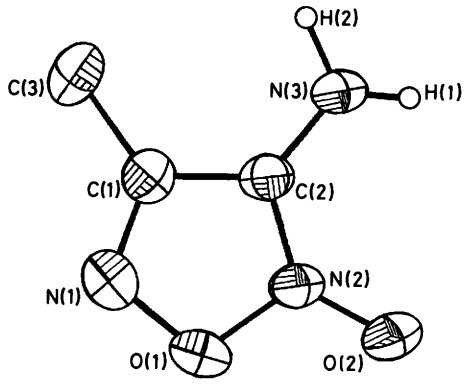

Figure 2. ORTEPII[3] projection of isomer (**1B**) on the plane through the five-membered ring; thermal ellipsoids are drawn at the 50% probability level

The geometry of the furazan oxide family is a stringent test for semiempirical calculations based on MINDO/3[4] and MNDO[13] approximations: there are in fact three interconnected N–O bonds for which these approaches present noticeable drawbacks. Preliminary tests on molecule (**1A**), using the MNDO approach, led to an unsatisfactory estimation of all the N–O lengths.*

On the other hand, MINDO/3 led to an acceptable trend for the N–O lengths, to a good estimation of bond angles, and to an overestimation of the value of the C–C bond. The failure of MNDO to reproduce the N–O lengths is probably related to the fact that no compound containing N–O bonds was included in the standard set of molecules used for the parametrization of MNDO.[13] On the other hand MINDO/3, which adopts different atomic parameters for a given atom linked to different atoms is, in this aspect, more versatile than MNDO which uses fixed atomic parameters.

Geometrical considerations. Starting from the *X*-ray data, full geometry optimization without any restriction was performed with the standard Fletcher–Powell routine[14] of the MINDO/3 program; for *ab initio* calculations a conjugate gradient method based on analytical first derivatives was used.[15] For (**4**) C_2 symmetry was fixed, following experimental evidence,[8] while for (**5**) and (**6**) C_s symmetry was imposed. In Figure 3 the geometries obtained by the two methods are reported, together with the experimental data.

The values for the C(1)–C(2) bonds are overestimated by MINDO/3, the mean deviation from the experimental values being 0.054 Å. Both C(1)–N(1) and C(2)–N(2) are well reproduced, the average deviation being 0.011 Å, though the computed values are systematically greater than those from the *X*-ray results, as also found for the furazan derivatives. Bonds N(1)–O(1) and N(2)–O(1) are underestimated, with a mean deviation of 0.069 Å. Nevertheless the observed difference between the two N–O distances in the ring, with a lengthening of the bond adjacent to the exocyclic N–O bond, is always accounted for. The deviation for the exocyclic N ⟶ O bond is only 0.026 Å, but again with a systematic underestimation. The bond angles of the furazan oxide ring are well accounted for by MINDO/3. Both the ring N–O–N and the exocyclic O–N ⟶ O angles are systematically overestimated by about 5°. In general MINDO/3 overestimates both C–C–NH_2 and C–C–Me angles, except for (**1B**) where C–C–NH_2 is underestimated. All these features are well

* Bond lengths in Å: *a* 1.449, *b* 1.397, *c* 1.350, *d* 1.306, *e* 1.356, *f* 1.205, *g* 1.486, *h* 1.396. Bond angles in degrees: *ab* 102, *bf* 131.1, *bc* 110.1, *cf* 118.8, *de* 109.0, *ea* 108.7, *eh* 122.0, *bg* 124.9.

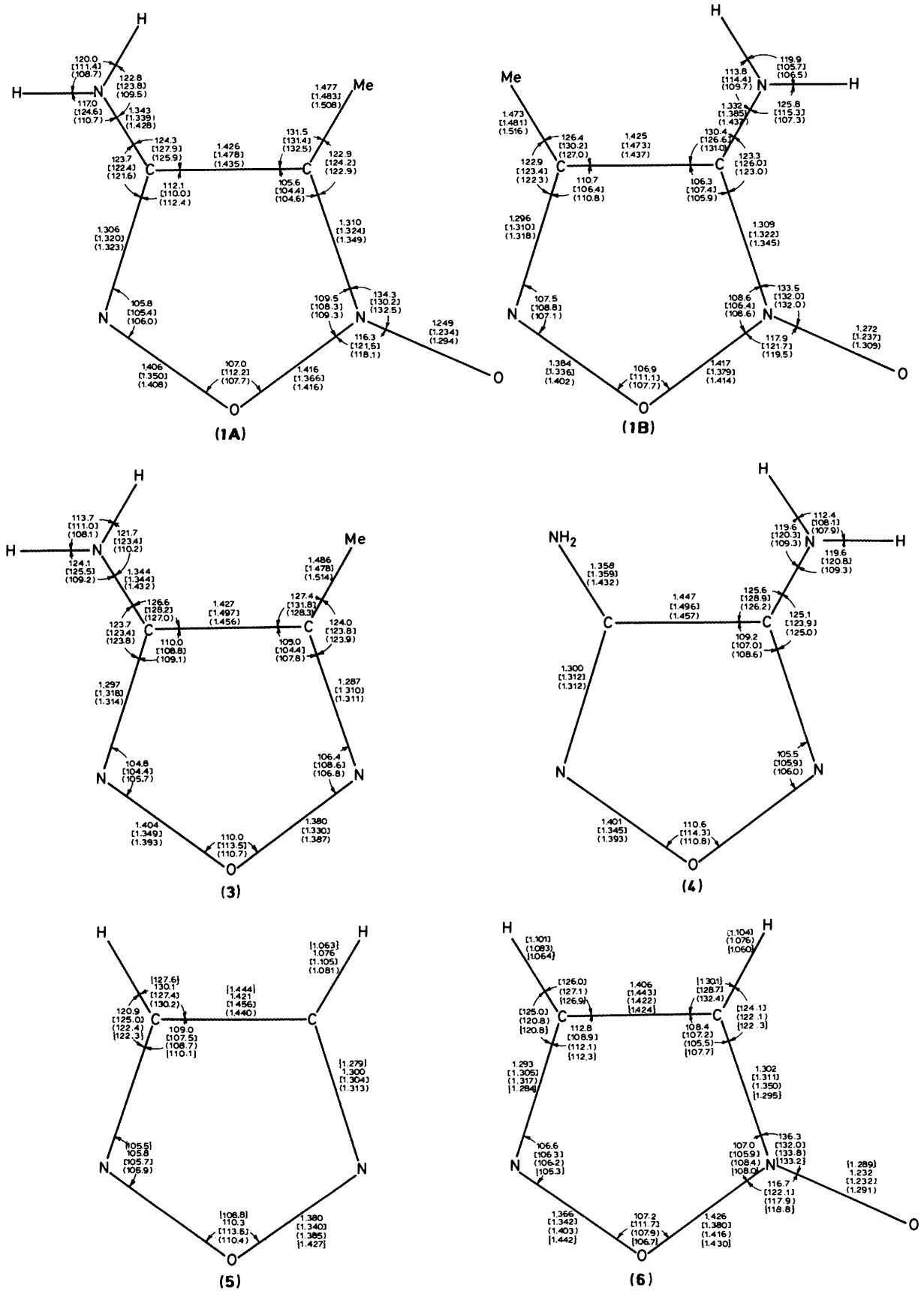

Figure 3. Diagrams showing the experimental geometries, the optimized geometries from MINDO/3 in square brackets, the optimized geometries from STO-3G in parentheses, and the optimized geometries from 3-21G in braces

Table 5. *Ab initio* and MINDO/3 (in parentheses) net charges; the 3-21G values are in square brackets. All the figures are in electrons × 10^4. The primed values refer to the primed atoms

	(1A)	(1B)	(3)	(4)	(5)	(6)
C(1)	445	952	677	1 551	−5	−250
	(−3 277)	(624)	(1 866)	(1 195)	(−105)	(−3 166)
					[154]	[968]
C(2)	1 825	1 376	1 563	1 551	−5	265
	(2 535)	(−1 683)	(−589)	(1 195)	(−105)	(690)
					[154]	[444]
N(1) or N(2)′	−1 510′	−1 135	−1 334′	−1 275	−832′	−1 037′
	(−177′)	(1 015)	(1 160′)	(155)	(1 057′)	(1 190′)
					[−1 750′]	[−1 851′]
O(1)	−435	−397	−648	−648	−546	−363
	(−3 558)	(−3 548)	(−2 413)	(−2 511)	(−2 474)	(−3 626)
					[−3 036]	[−2 541]
N(2) or N(1)′	820′	568	−994′	−1 275	−832′	938′
	(9 027′)	(8 290)	(−235′)	(155)	(1 057′)	(1 190′)
					[−1 750′]	[529′]
O(2)	−2 058	−2 327				−1 916
	(−5 804)	(−5 805)				(−5 784)
						[−4 198]
C(3) or H′	−1 776	−1 811	−1 830		1 000′	1 193′
	(1 740)	(872)	(1 145)		(285′)	(1 207′)
					[6 880′]	[3 389′]
N(3) or H′	−3 786	−3 721	−3 784	−3 800	1 000′	1 170′
	(−1 641)	(−864)	(−1 750)	(−1 551)	(285′)	(462′)
					[6 880′]	[3 261′]

rationalized in terms of the known tendency of NDO, based methods to overestimate non-bonded interactions between atoms at a distance close to the sum of their van der Waals radii. The geometries of the furazan and furazan oxide rings are well accounted for by the *ab initio* STO-3G basis set. The largest discrepancy occurs with the length of the exocyclic N ⟶ O bond, which, on average, is overestimated by 0.041 Å. The predictions of local geometry of the NH_2 substituent by MINDO/3 and *ab initio* methods shows clear differences, the former predicting a lesser degree of pyramidalization than the latter. Comparison with *X*-ray data must be made with some caution, because in the crystal the NH_2 group is involved in strong intermolecular contacts as described in the preceding section. Optimization of the geometries employing STO-3G and 3-21G basis sets has also been performed for furazan (**5**) and furazan *N*-oxide (**6**), keeping C_S symmetry. Furazan *N*-oxide has not yet been synthesized, and an 'experimental geometry' was constructed from that of the phenylfurazan *N*-oxide isomers described in reference 1. While the C–N bonds become shorter on passing from STO-3G to 3-21G, an increase is observed for the ring N–O bonds; the difference between these two N–O bonds, however, is smaller than for the semiempirical results and a similar trend is observed for furazan (**5**).

Electronic considerations. The charge distributions for all molecules are reported in Table 5, with a comparison between the values of the net charges from *ab initio* and semiempirical calculations. We are aware that these values, obtained from an arbitrary partitioning of the electron density, must be used with some caution but they are often used as indicators in structure–activity relationships. A one-to-one comparison between the two sets of data shows significant differences. In particular, as is well known,[4] MINDO/3 inverts the polarity of the methyl group with respect to the *ab initio* results. Further, the MINDO/3 value for the ring nitrogen not linked to the exocyclic oxygen is always positive [except for (**1A**)] while the reverse is found at *ab initio* level. This difference does not depend on the presence of the methyl group as a substituent, since the same trend is observed for molecules (**5**) and (**6**). In spite of these differences, both methods indicate a similar overall description

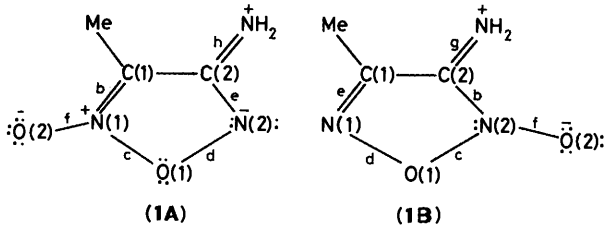

Scheme 1.

of the electronic effects of the substituents. In particular, an analysis of the charges on N(2) in isomers (**1A**) and (**1B**) shows apparent consistency of both *ab initio* and MINDO/3 values, in a simple valence-bond framework, with the two possible limit forms shown in Scheme 1.

Two sets of calculations were performed: one without any geometrical constraint and the other with the amino group constrained to be coplanar with the five-membered ring (the corresponding *ab initio* values are given in parentheses hereinafter). At the *ab initio* level, the negative charge on N(2) is in fact −0.1510 (−0.1679) for (**1A**), with respect to the value of −0.1135 (−0.1054) for N(1) in (**1B**), while values of 0.0820 (0.0828) and 0.0568 (0.0286) were found for the charges on N(1) for (**1A**) and on N(2) for (**1B**). The values in parentheses are in agreement with a higher degree of conjugation of the substituent with the ring. The MINDO/3 approach gave the same trend. The lengthening in bond *d* observed in (**3**) and in (**1A**) can be explained also in terms of increased repulsion between the lone pairs of N(2) and O(1).

From Mulliken population analysis[16] at the *ab initio* level, a value of 0.4478 (0.443) for bond *e* in isomer (**1A**) was found, to be compared with a value of 0.4594 (0.461) for isomer (**1B**), showing less double-bond character in the first than in the second, in agreement with the *X*-ray results. The bond-order values for the exocyclic bonds *f* are also consistent with Scheme 1 and with experimental results, being 0.2418 (0.242) for (**1A**) and 0.2228 (0.200) for (**1B**). The other bond-order values agree

Table 6. Bond-order values from *ab initio* and MINDO/3 (in parentheses); 3-21G values in square brackets. All figures are in electrons × 10^3

	(1A)	(1B)	(3)	(4)	(5)	(6)
a	451	448	375	419	436	461
	(1 031)	(1 043)	(990)	(960)	(1 079)	(1 105)
					[319]	[296]
b	422	424	471	465	469	420
	(1 469)	(1 500)	(1 610)	(1 650)	(1 735)	(1 517)
					[386]	[1 658]
c	210	212	235	232	237	212
	(918)	(860)	(998)	(1 010)	(1 039)	(894)
					[184]	[124]
d	221	224	232	232	237	224
	(974)	(1 050)	(1 060)	(1 010)	(1 039)	(1 009)
					[184]	[172]
e	449	459	463	465	469	459
	(1 561)	(1 690)	(1 710)	(1 650)	(1 735)	(1 728)
					[386]	[362]
f	242	223				245
	(1 286)	(1 200)				(1 278)
						[160]
g	380	393	385	352	393	397
	(962)	(1 030)	(1 100)	(1 050)	(912)	(907)
					[367]	[366]
h	358	374	354	352	393	393
	(1 112)	(969)	(968)	(1 050)	(912)	(915)
					[367]	[370]

Table 7. MINDO/3 heats of formation, *ab initio* total energies, ionization potentials, and total dipole moments. MINDO/3 values in parentheses and 3-21G values in square brackets

	Heat of formation (kJ mol^{-1})	Total energy (a.u.)[a]	I_p/eV[b]	Dipole (Debyes)[c]
(1A)	−118.031	−423.882 164	6.276	4.248
			(9.020)	(5.695)
		[−426.957 288]	[9.448]	[6.537]
(1B)	−95.180	−423.877 076	6.097	3.693
			(8.839)	(3.611)
		[−426.955 166]	[9.354]	[5.944]
(3)	−59.848	−350.145 675	8.449	3.800
			(7.151)	(3.855)
		[−352.615 141]	[10.509]	[5.355]
(4)	−70.795	−365.879 997	8.298	3.298
			(7.915)	(4.755)
		[−368.511 293]	[10.362]	[4.786]
(5)	78.910	−257.233 398	10.01	2.967
			(9.206)	(2.790)
		[−259.067 077]	[12.29]	[4.548]
(6)	22.671	−330.968 065	6.685	3.289
			(9.234)	(4.339)
		[−333.406 273]	[10.04]	[5.521]

[a] 1 a.u. = 2 625.54 kJ mol^{-1}. [b] 1 eV = 27.21 kJ mol^{-1}. [c] 1 Debye = 3.34 × 10^{-30} C m.

Table 8. Pyramidalization energy E_P, torsional energy E_t, and Fourier coefficients (V_1, V_2, V_3) of the torsional curves. MINDO/3 data in parentheses

	(1A)	(1B)	(3)	(4)
E_P	13.7	25.8	17.8	22.7
	(4.1)	(12.4)	(4.5)	(5.2)
E_t	40.35	8.1	31.4	31.9
	(24.30)	(−2.8)	(19.8)	(14.9)
V_1	0.098	−0.111	0.065	−1.159
	(0.905)	(−0.280)	(0.842)	(0.586)
V_2	40.46	8.44	31.56	31.36
	(19.90)	(−3.56)	(16.04)	(11.15)
V_3	0.098	−0.111	0.065	−1.160
	(−1.751)	(−0.129)	(−1.487)	(1.032)

with the usual description of the furazan oxide ring: *d* is a normal single bond [0.2207/0.2244 (**1A**)/(**1B**)], and *c* is weakened [0.2104/0.2121 (**1A**)/(**1B**)]. In fact bond *d* has an order population close to 0.2319 in (**4**) or 0.233 in (**3**). To be compared with an average value of 0.4640 for the C–N bonds in (**3**) and (**4**), values of 0.4487 for bond *e* and 0.4240 for bond *b* were obtained for isomers (**1A**) and (**1B**), respectively, thus showing that, expecially for (**1A**), the electronic effects of the NH_2 group are better accommodated in the furazan oxide system than in furazan. The same trend as just described at the *ab initio* level was found with MINDO/3 (see Table 6), which employs a different partition of the density matrix.[17] The total dipole moment for these compounds is reported in Table 7; the values in square brackets for (**1A**), (**1B**), (**3**), and (**4**) were obtained using a 3-21G basis set on the STO-3G- optimized geometry. All methods predict that these molecules have high dipole moments, making them suitable as 'urea equivalent' groups.[2] Isomer (**1A**) is predicted to be more stable than (**1B**) by 22.9 kJ mol^{-1}, using MINDO/3 heats of formation and by 13.4 kJ mol^{-1} when total *ab initio* energy is employed. Some differences appear in the ionization potentials. The STO-3G data for furazan oxides are about 3 eV lower than those for furazans, while with 3-21G the difference is reduced to *ca.* 1 eV, indicating that an electrophilic agent can more easily attack the furazan oxide system than the corresponding furazan ring. The absence of experimental ionization potentials (to our knowledge) and the contradictory indication of MINDO/3 do not allow us to draw any definitive conclusion.

Conformational analysis. Conformational analyses were performed concerning the energy involved both in the pyramidalization of the NH_2 group and in the rotation around the C–NH_2 bond. In Table 8 the main results of these analyses are reported. As already mentioned, full optimization of the geometry at *ab initio* STO-3G level overestimates the degree of pyramidalization of the amino group: the local symmetry of the NH_2 moiety (see Figure 3) assumes a nearly total sp^3 character.

Table 9. Bond lengths (in Å) ($\times 10^3$) of the furazan oxide ring in disubstituted derivatives; $\delta_{max.}$ is the difference between the longest and the shortest

		a	e	b	d	c	f
3-Me-4-NO_2	(A)[a]	1 401	1 288	1 332	1 367	1 479	1 220
3-NO_2-4-Ph	(B)[b]	1 410	1 314	1 316	1 386	1 440	1 204
3-Me-4-$PhSO_2$	(A)[c]	1 417	1 307	1 313	1 372	1 465	1 237
3-$PhSO_2$-4-Me	(B)[c]	1 409	1 288	1 325	1 380	1 423	1 224
3-Me-4-NH_2NHCO	(A)[d]	1 413	1 306	1 317	1 358	1 450	1 229
3-NH_2NHCO-4-Me	(B)[d]	1 422	1 307	1 326	1 388	1 427	1 231
3-Me-4-NH_2CO	(A)[e]	1 419	1 307	1 324	1 375	1 445	1 240
3-NH_2CO-4-Me	(B)[e]	1 423	1 304	1 324	1 384	1 428	1 232
3-Me-4-$CONMe_2$	(A)[g]	1 411	1 299	1 310	1 368	1 447	1 242
3-$CONMe_2$-4-Me	(B)[f]	1 424	1 301	1 311	1 384	1 436	1 232
3-Ph-4-Cl	(A)[h]	1 420	1 301	1 326	1 375	1 452	1 219
3-Cl-4-Ph	(B1)[h]	1 416	1 317	1 305	1 366	1 452	1 236
3-Cl-4-Ph	(B2)[h]	1 413	1 307	1 317	1 384	1 433	1 229
3-Ph	(A)[i]	1 417	1 289	1 318	1 369	1 439	1 239
4-Ph	(B)[i]	1 396	1 307	1 302	1 377	1 435	1 231
3-Me-4-Pr^iO_2CNH	(A1)[j]	1 415	1 308	1 312	1 398	1 436	1 242
3-Me-4-Pr^iO_2CNH	(A2)[j]	1 417	1 307	1 314	1 390	1 431	1 238
3-Pr^iO_2CNH-4-Me	(B)[j]	1 407	1 308	1 302	1 391	1 442	1 240
3-Me-4-NH_2	(A)	1 426	1 306	1 310	1 406	1 416	1 249
3-NH_2-4-Me	(B)	1 425	1 296	1 309	1 384	1 417	1 272
Mean		1 415	1 303	1 316	1 380	1 440	1 234
σ		8	8	8	12	15	13
$\delta_{max.}$		24	29	30	48	63	68

[a] F. Cameron and A. A. Freer, *Acta Crystallogr., Sect. B*, 1974, **30**, 354. [b] R. Calvino, A. Gasco, A. Serafino, and D. Viterbo, *J. Chem. Soc., Perkin Trans. 2*, 1981, 1240. [c] M. Calleri, G. Chiari, A. Chiesi Villa, A. Gaetani Manfredotti, C. Guastini, and D. Viterbo, *Acta Crystallogr., Sect. B*, 1976, **32**, 1032. [d] M. Calleri, G. Chiari, G. Germain, and D. Viterbo, *Acta Crystallogr., Sect. B*, 1973, **29**, 1618. [e] M. Calleri, G. Chiari, A. Chiesi Villa, A. Gaetani Manfredotti, C. Guastini, and D. Viterbo, *Acta Crystallogr., Sect. B*, 1975, **31**, 2384. [f] M. Calleri, D. Viterbo, A. Gaetani Manfredotti, and C. Guastini, *Cryst. Struct. Commun.*, 1974, **3**, 269. [g] A. Chiesi Villa, C. Guastini, M. Calleri, and G. Chiari, *Cryst. Struct. Commun.*, 1974, **3**, 265. [h] G. Chiari, D. Viterbo, and R. Calvino, *Acta Crystallogr., Sect. B*, 1982, **38**, 3045. [i] Ref. 1. [j] M. Calleri, G. Chiari, A. Chiesi Villa, A. Gaetani Manfredotti, C. Guastini, and D. Viterbo, *Acta Crystallogr., Sect. B*, 1977, **33**, 479.

MINDO/3 gives a more realistic description of the hybridization of the amino group and, apart from isomer (**1B**), the degree of pyramidalization increases smoothly, in the series (**1A**) < (**3**) < (**4**). Experimental data follow the same trend, even though the intermolecular network of hydrogen bonds can obscure these electronic effects. In order to determine the energy required for achieving planarity of the amino group, reoptimization of the geometries was carried out keeping the following parameters fixed: bond angles C–N–H and H–N–H at 120°, torsion angles C–C–N–H and N–C–N–H at 0° and O–N–C–N at 180°. These constraints keep the substituent sp^2-hybridized, thus maximizing the conjugative effects with the ring. For the molecule (**4**) only one of the two amino groups was constrained. All other degrees of freedom were fully relaxed, and E_P was computed as $E(NH_2$ pyramidal) − $E(NH_2$ planar). Both theoretical methods give the same trend: E_P increases smoothly in the series (**1A**) < (**3**) < (**4**) < (**1B**). Starting from these geometries a rotation of the amino group around the C–NH_2 bond, optimizing for each point only the C–NH_2 bond length, was performed at the *ab initio* minimal basis set level. Scanning of the N–C–N–H torsion angle was carried out in 30° steps, assuming a symmetrical behaviour beyond 90°. The first three coefficients of a truncated Fourier representation of the curves[18] are reported in Table 8. The same analysis was carried out at MINDO/3 level, but here full optimization of the geometries was applied at each point. The high values of V_2 indicate a predominant conjugative effect; in only (**1B**) and (**4**) is the relative contribution of V_1 and V_3 higher, showing that electrostatic interactions are present. *Ab initio* results predict an increase of the torsion energy E_t in the series (**1B**) < (**3**) ≈ (**4**) < (**1A**), whereas MINDO/3 gives (**1B**) < (**4**) < (**3**) < (**1A**). Despite the stronger electronic interaction in the furazan oxide (**1A**), its torsion curve is similar to those of (**3**) and (**4**). On the other hand, both methods show anomalous behaviour of the isomer (**1B**). In this isomer, in fact, electrostatic interactions between the amino substituent and the exocyclic N ⟶ O bond are important. A careful analysis of the geometries of this fragment shows that MINDO/3 fully optimized geometry gives a higher degree of pyramidalization and a partial rotation of the NH_2 group, with respect to isomer (**1A**). This effect is due to the overestimation by MINDO/3 of the non-bonded repulsions with a consequent underestimation of hydrogen-bond energy.[19] In fact the distance N(3) • • • O(2) decreases by 0.1 Å when planar geometry is imposed, while the shortest O(2) • • • H distance decreases by 0.4 Å, and as a consequence conjugative effects by the substituent are obscured. The local geometry obtained at *ab initio* level reveals that H(1) tends to lie in the O(2)–N(2)–C(2)–N(3) plane, with formation of a penta-atomic ring through a weak hydrogen bond. Experimental *X*-ray data seem to be consistent with the *ab initio* prediction of formation of an intramolecular contact. The high value of E_P for (**1B**) can be rationalized by noting that, when planarity is imposed, the geometry becomes less favourable for the formation of the H bond (the N–H • • • O angle decreases from 105° to 96°). On the other hand the small value of E_t is the consequence of a compromise between the conjugative barrier and the weakening of the H-bond interaction.

Concluding remarks. Table 9 gives the bond lengths of the furazan oxide ring in most disubstituted derivatives studied so far. On the basis of *X*-ray analyses and theoretical calculations it has been shown that the presence of a $+I$ substituent, such as the amino group, influences the electronic and geometrical structure of the furazan and furazan oxide rings. Some features may be accounted for by the simple valence-bond picture of Scheme 1. Most previously analysed furazan oxide isomers have $-I$ substituents and in this case the geometrical results are consistent with Scheme 2. In particular, for all pairs of isomers, the difference between the two ring N–O bonds is about twice as

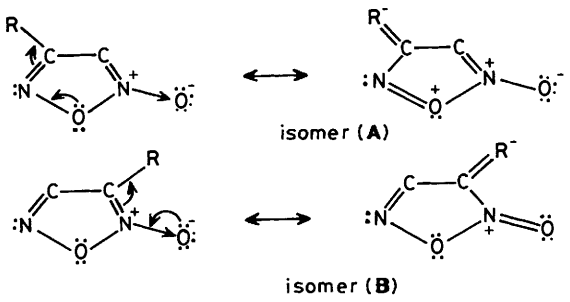

Scheme 2.

great in isomer (**A**) than in (**B**). Besides, as already pointed out, the exocyclic N ⟶ O bond is always significantly shorter than in the NH_2 derivatives. The consistency of Schemes 1 and 2 with the geometry applies only to the N–O bonds, while the N=C–C=N moiety seems to be rather insensitive to the nature of the substituents as shown by the σ and $\delta_{max.}$ values in Table 9. Indeed the N–O–N ⟶ O moiety is rich with unshared electron pairs and therefore more sensitive to electrostatic effects, which seem to play a major role in defining the resulting geometry.

Experimental

Both compounds were supplied by Professor A. Gasco and his co-workers. The isomer (**1A**) was crystallized from ethyl acetate as thick colourless plates; (**1B**) was crystallized from chloroform as colourless needles.

For both crystals the space groups and the unit-cell parameters were derived from diffractometer measurements. The intensities for (**1B**) were collected with a Philips PW 1100 four-circle diffractometer, using graphite-monochromated Cu-K_α radiation and the θ–2θ scan technique with variable speed. The intensities for (**1A**) were measured by ω-scan with variable speed with a Nicolet R3 diffractometer using graphite-monochromated Mo-K_α radiation. Lorentz and polarization corrections were applied to yield structure amplitudes. The unit-cell parameters were determined and refined from 25 automatically centred reflections.

Both structures were solved by direct methods. For (**1B**) the SHELXTL system [20] was used; that for (**1A**) was solved by the RANTAN [21] routine of the SHELXTL system.[22] The *E*-maps computed with the most consistent set of phases revealed in both cases all non-hydrogen atoms.

The structures were refined, using the SHELXTL system, by full-matrix least-squares cycles with anisotropic temperature factors for the non-hydrogen atoms. The hydrogen atoms were located on difference-Fourier maps and refined with geometric constraints and isotropic temperature factors. The methyl group of isomer (**A**) showed a disordered disposition of the H-atoms in two minimum-energy positions rotated by approximately 60°. The weighting scheme used in the final cycles is $1/[\sigma^2(F_0) + GF_0^2]$, where σ is the standard deviation of $|F_0|$ and G an adjustable parameter. At convergence $R_w = 0.066$ with G = 0.0081 for (**1B**) and $R_w = 0.045$ with $G = 0.0005$ for (**1A**).

Crystal Data.—(**1A**): $C_3H_5N_3O_2$, $M = 115.1$, monoclinic, space group $P2_1/n$, $a = 10.805(3)$, $b = 5.860(2)$, $c = 8.567(2)$ Å, $\beta = 106.63(3)$, $V = 519.8(2)$ Å^3, $Z = 4$, $D_c = 1.47$ Mg m^{-3}, $F(000) = 240$, Cu-K_α radiation, $P = 1.541\,78$ Å, $\mu = 0.97$ mm^{-1}, $R = 0.047$ for 875 reflections ($3° < \theta < 65°$).

(**1B**): $C_3H_5N_3O_2$, $M = 115.1$, monoclinic, space group $P2_1/n$, $a = 6.360(1)$, $b = 6.503(1)$, $c = 12.302(2)$ Å, $\beta = 94.98(2)$, $V = 506.9(2)$ Å^3, $Z = 4$, $D_c = 1.51$ Mg m^{-3}, $F(000) = 240$, Mo-K_α radiation, $P = 0.710\,69$ Å, $\mu = 0.12$ mm^{-1}, $R = 0.038$ for 933 reflections ($1° < \theta < 27.5°$) having $I > 2\sigma(I)$.*

Acknowledgements

We acknowledge the support of the CSI Piemonte computing centre in allowing us free computing time. We also thank Professor A. Gasco and his co-workers (Dipartimento di Scienza e Tecnologia del Farmaco, Torino University) for providing the samples and for discussions.

References

1 M. Calleri, G. Ranghino, P. Ugliengo, and D. Viterbo, *Acta Crystallogr., Sect. B*, 1986, **42**, 84.
2 G. Sorba, R. Calvino, A. Defilippi, A. Gasco, and M. Orsetti, *Eur. J. Med. Chem.-Chim. Ther.*, 1985, **20**, 571.
3 C. K. Johnson, ORTEPII, 1976, Report ORNL-5138, Oak Ridge National Laboratory, Tennessee.
4 R. C. Bingham, M. J. S. Dewar, and D. H. Lo, *J. Am. Chem. Soc.*, 1975, **97**, 1285; 1977, **99**, 1294, 1302.
5 W. J. Hehre, R. F. Stewart, and J. A. Pople, *J. Chem. Phys.*, 1969, **51**, 2657.
6 J. S. Binkley, J. A. Pople, and W. J. Hehre, *J. Am. Chem. Soc.*, 1980, **102**, 939.
7 D. Viterbo and A. Serafino, *Acta Crystallogr., Sect. B*, 1978, **34**, 3444.
8 A. S. Batsanov and Y. T. Struchkov, *Zh. Strukt. Khim.*, 1985, **26**, 65.
9 E. Saegebarth and A. P. Cox, *J. Chem. Phys.*, 1965, **43**, 166.
10 'MOPAC: A General Molecular Orbital Package (IBM Version),' J. J. P. Stewart, QCPE 464, Dewar Group, University of Texas, Austin, Texas 78712.
11 J. S. Binkley, R. A. Whiteside, R. Krishnan, R. Seeger, D. DeFrees, H. Schlegel, S. Topiel, L. Kahn, and J. A. Pople, QCPE, 1981, **13**, 406; P. N. Van Kampen, G. F. Smits, F. A. A. M. De Leeuw, and C. Altona, QCPE, 1982, **14**, 437.
12 GAUSSIAN82, J. S. Binkley, M. J. Frisch, D. J. DeFrees, K. Raghavachari, R. A. Whiteside, H. B. Schlegel, E. M. Fluder, and J. A. Pople, Department of Chemistry, Carnegie-Mellon University, Pittsburgh.
13 M. J. S. Dewar and W. Thiel, *J. Am. Chem. Soc.*, 1977, **99**, 4899, 4907.
14 R. Fletcher and M. J. D. Powell, *Comput. J.*, 1963, **6**, 163.
15 H. B. Schlegel, *J. Comput. Chem.*, 1982, **3**, 214.
16 R. S. Mulliken, *J. Chem. Phys.*, 1955, **23**, 1833.
17 D. R. Armstrong, P. G. Perkins, and J. J. P. Stewart, *J. Chem. Soc., Dalton Trans.*, 1973, 838.
18 L. Radom, W. J. Hehre, and J. A. Pople, *J. Am.. Chem. Soc.*, 1972, **94**, 2371.
19 T. J. Zielinski, D. L. Breen, and R. Rein, *J. Am. Chem. Soc.*, 1978, **100**, 6266; G. Klopman, P. Andreozzi, A. J. Hopfinger, O. Kikuchi, and M. J. S. Dewar, *ibid.*, p. 6267; S. N. Mohammad and A. J. Hopfinger, *Int. J. Quantum Chem.*, 1982, **22**, 1189.
20 G. M. Sheldrick, 'SHELXTL, 1981. An Integrated System for Solving, Refining and Displaying Crystal Structures from Diffraction Data, revision 3,' University of Göttingen, Federal Republic of Germany.
21 Yao Jia-Xing, *Acta Crystallogr., Sect. A*, 1981, **37**, 642.
22 G. M. Sheldrick, 'SHELXTL, 1983. An Integrated System for Solving, Refining and Displaying Crystal Structures from Diffraction Data, revision 4,' University of Göttingen, Federal Republic of Germany.

* *Supplementary data* (see sections 4.0 and 5.63 of Instructions for Authors, in the January issue). H-Atom co-ordinates and thermal parameters have been deposited at the Cambridge Crystallographic Data Centre. Lists of cartesian co-ordinates of the optimized geometry for all studied compounds are available as Supplementary Publication No. SUP 56707 (5 pp.) from the British Library.

Received 11*th May* 1987; *Paper* 7/828